Arab J Geosci (2016) 9:552
DOI 10.1007/s12517-016-2576-6

ORIGINAL PAPER

Evaluation of rain gauge network in arid regions using geostatistical approach: case study in northern Oman

Mohammed Haggag[1,2] · **Ahmed A. Elsayed**[2] · **Ayman G. Awadallah**[2,3]

Received: 9 January 2016 / Accepted: 6 June 2016

Abstract A geostatistical approach based on ordinary kriging is presented for the evaluation and the augmentation of an existing rain gauge network. The evaluation is based on estimating the percentage of the area that achieves a targeted level of acceptable accuracy. The variances of kriging estimation erros at un-gauged locations were assumed to be normally distributed. Kriging estimation erros with a probability that equals to or exceeds a given threshold value of acceptance probability were assumed to have satisfactory accuracies. The percentage of the area that achieved the targeted probability of acceptance is delineated and used to judge the overall performance of the existing rain gauge network. A study area in northern Oman located in Sohar governorate is selected as the pilot case. The area has 34 rain gauges and it is characterized by a terrain surface that varies from coastal plain to mountains. For a threshold value of 0.85, and 0.90 of acceptance probability, the existing network achieved area of acceptable probability of 88.71 and 77.72 %, respectively. For a success criterion of 80 %, the existing rain gauge network indicated acceptable performance for acceptance probability threshold of 0.85 and inadequate performance is noticed in the case of probability threshold of 0.90, which necessitated further network augmentation. A sequential algorithm for ranking and prioritization of the existing rain gauges is used to classify the existing rain gauges into base and non-base rain gauges. The base rain gauge network for mean annual rainfall comprised about 29 of the existing rain gauges. The identified non-base rain gauges were sequentially relocated to achieve higher levels of percentage of area with acceptable accuracy. The percentage of area with acceptable accuracy increased from 88.71 % for the original rain gauge network to about 94.51 % for the augmented network by adding four rain gages at probability acceptance threshold of 0.85. It also increased from 77.72 % for the existing network to 90.50 % for the augmented rain gauge network at acceptance threshold of 0.9.

Keywords Rain gauge network · Geostatistics · Ordinary kriging · Sequential algorithm · Semivariogram · Oman

This article is part of the Topical Collection on *Water Resources in Arid Areas*

✉ Mohammed Haggag
mohammed.abou-elhaggag@dar.com

[1] Department of Irrigation and Hydraulics, Faculty of Engineering, Cairo University, Dokki, Giza 12613, Egypt

[2] Dar Al-Handasah, Shair and Partners, Giza, Egypt

[3] Civil Engineering Department, Faculty of Engineering, Fayoum University, Fayoum, Egypt

Introduction

Countries in the Middle East region are particularly suffering from the lack of adequate rain gauge network. The vulnerability of these countries to potential climate change effects combined with the already existing water scarcity and hyper aridity conditions suggest more investments in rainfall monitoring for efficient management of the limited water resources. The hydrometeorological characteristics of the Sultanate of Oman has a tendency to produce short duration high intensity storms giving rise to flash floods with consequent damage and disruption to properties.

The optimum rain gauge network is the one that eliminates serious deficiencies in the utilization, development, and management of water resources. In un-gauged catchments, the rain gauge network should be developed as rapidly as possible, incorporating existing gauges and providing a framework for future expansion to meet the information requirements of

Published online: 11 July 2016

specific water uses. The concept of rain gauge network density is intended to serve as a general guideline if specific guidance is lacking. As such, the design densities must be adjusted to reflect actual socioeconomic and physio-climatic conditions. Computer-based mathematical analysis techniques should also be applied, where data are available, to optimize the rain gauge network density required to satisfy specific needs.

Modern rain gauges are capable of providing rainfall rates in real time and at very fine resolution in time. However, the spatial variation of rainfall is still difficult to be characterized without a rain gauge network of adequate density in space. The latest advances in satellite imagery, weather satellites, and remote sensing appear to have the potential to provide full spatial coverage of rainfall estimates. Satellite-based monitoring techniques have also caused deterioration of rain gauge networks in some cases (Ali et al. 2005). In fact, data provided by satellite-based techniques are still incapable to provide accurate rainfall estimates at a spatial resolution that matches rain gauge measurements. In addition, the mathematical algorithms used to retrieve rainfall data from satellite observations still need to be calibrated and validated using ground-based rainfall measurements, i.e., by rain gauges. In some applications, the satellite images were even coupled with rain gauge observations to produce better estimates of point or areal rainfalls (Krajewski 1987).

The objective of having a rain gauge network is to properly capture the rainfall and explain its spatial and temporal variabilities within a certain area. The rainfall variability depends on topography, wind, direction of storm movement, and type of storm. The locations and spacing between gauges depend not only on the above-mentioned factors but also upon the purpose of the rain gauge network, accessibility, ease of maintenance, topographical aspects, etc. Some of the rain gauge networks are intended for applications related to water resources planning and management (e.g. water balance studies, storage dams, and groundwater recharge). The other type of rain gauge network is the one intended for use in storm drainage and flood protection purposes, i.e. hydrological studies required for hydraulic design of bridges, culverts, channels, storm water networks, etc. The main data required from the first type is the long-term averaged rainfall data, e.g., mean monthly and mean annual rainfall depths. Whereas the data needed from the second type of rain gauge network is the high-temporal resolution records (hourly and sub-hourly records) which are crucial to define the storm pattern and consequently the design rainfall intensity. Some rain gauge network could be intentionally designed to serve both purposes of water resources planning and drainage design applications. Hence, a methodology for performance evaluation and augmentation of an existing rain gauge network is crucial. It can help to understand the capability of an existing rain gauge network in achieving its purpose and the quality of the data it provides.

The literature review includes several attempts to study the rain gauge network design. Langbein (1960) suggested that a reasonable minimum rain gauge density should be above 2 gauges per 1000 km^2. The World Meteorological Organization, WMO (2008), recommends certain densities of rain gauges to be adopted for different types of catchments. The World Meteorological Organization (WMO 2008) minimum rain gauge network criterion distinguishes between two classes of rain gauges, the non-recording and the recording rain gauges. In flat terrain of temperate zones, 500 km^2 per non-recording gauge and 5000 km^2 per recording gauge are recommended. For small mountainous islands with irregular precipitation, 25 km^2 per non-recording gauge and 250 km^2 per recording gauge are recommended. The recommended rain gauges' densities by WMO are not applicable to the great deserts (Sahara, Gobi, Arabian, etc.) and great ice fields (Antarctic, Greenland, and the Arctic islands) that have no organized hydrographic networks.

In contrast to the above-mentioned descriptive guidelines for the design and evaluation of a rain gauge network, there are more data driven-based techniques. These methods utilize the available rainfall records from the existing rain gauges in a certain area to provide basis for evaluation and augmentation of the rain gauge network. Statistical techniques are commonly adopted for rain gauge network design and evaluation. Patra (2001) used simple statistical approaches, e.g., the coefficient of variation and the allowable percentage of error, to estimate the optimal number of rain gauges. However, the design of rain gauge network does not only involve the determination of the number of gauges, but also the location of the gauges is also necessary. Both number and locations are necessary to achieve the required accuracy by providing observation that depicts the temporal and spatial variations of rainfall in a certain context.

Geostatistical techniques proved to have many potential applications in hydrological research; in particular, the optimal estimation of the average value over a region using the variance reduction concept. Several applications of rain gauge evaluation and optimization using geostatistics are reported in the literature, including (Cheng et al. 2008; Mahmoudi-Meimand et al. 2015; Kar et al. 2015; Adhikary et al. 2015a; Seo et al. 2015; Hui-Chung et al. 2011; Chebbi et al. 2011; St-Hilaire et al. 2003; Tsintikidis et al. 2002; Pardo-Igúzquiza, 1998; Kassim and Kottegoda 1991; Bastin et al. 1984). Another major approach for the design and evaluation of the rain gauge networks is the information entropy (Mahmoudi-Meimand et al. 2015; Hongliang et al. 2015; Hui-Chung et al. 2011; Chen et al. 2006). The nature of the objective function used for optimization of rain gauge network could be any of geostatistical-based (variance-based), entropy-based, fractal-based, or distance-based techniques. In this paper, we adopt the geostatistical approach which has the merit of taking the spatial nature of the rainfall phenomena and observations into consideration and using the semivariogram as a measure to

quantify the spatial variability. The geostatistical approaches are a well-understood way of capturing spatial variation compared to other methods. A detailed presentation of geostatistical theories can be found in Webster and Oliver (2007).

Most of the geostatistical applications for rain gauge network design considered only annual or monthly time steps for network evaluation, e.g. (Lloyd 2005; Vicent-Serrano et al. 2003). High-resolution time scale of hourly data is also reported (Haberlandt 2007). The analysis of the spatial distribution of hourly and daily rainfall is rather difficult mainly because of intermittence and large variability (Carrera-Hernandez and Gaskin 2007). Rain gauge network optimization aims at providing correct description of the spatial rainfall estimation. The performance of a certain network focuses on minimizing the estimation variance of the areal rainfall and not that of point rainfalls across the area of concern. In some cases using areal rainfall to force hydrological and rainfall-runoff simulation models may be adequate for flood simulation. This is because catchments act as low-pass filters and the necessary intervals for rainfall measurements in time and in space may be determined by the variability in the discharge simulated at the outlet of the catchment (Eagleson 1967). Monitoring of localized high-intensity rainfall is immensely important in catchments that have steep slopes with quick response to local rainfall. In this case, rain gauge network shall be installed tailoring to such needs.

The main objective of this paper is to analyze, and evaluate the performance, and provide augmentation recommendations of an existing rain gauge network located in the northern part of Sultanate of Oman. The methodology is based on the well-known ordinary Kriging approach. A sequential prioritization algorithm is developed to prioritize the existing rain gauges and hence determine the base rain gauges which must be kept in their locations and the non-base gauges which can be eliminated or relocated.

Following this "Introduction" section, the "Study area" section provides description of the study area and data included in the paper. The "Materials and methods" section provide details of the material and methods including data preparation, the governing equations ordinary kriging, cross-validation methods, and description of the prioritization sequential algorithm. In the "Results and discussion" section, we present the results of the ordinary kriging, rain gauge network evaluation and augmentation. Finally, the "Conclusions" section summarizes the main findings of the paper.

Study area

A case study of rain gauge network in Sultanate of Oman is used to represent the conditions in arid regions. Oman lies on the southeast corner of the Arabian Peninsula between longitudes 55.50 E to 60.0 E and latitudes 21.50 N to 26.50 N. It occupies a total land area of about 309,500 km^2 and includes different terrains that vary from highlands, wadies, inland plains, and coastal plains. Only the Al Hajar Mountains in the north and the Dhofar Mountains in the south, have regular rainy seasons with substantial rainfall. Rainfall in the rest of the country is low and irregular. Heavy rains can occur, sometimes delivering all the rainfall amount of the year in a single shower event, causing violent floods. Mean annual rainfall is less than 50 mm in the interior regions which cover two thirds of the country and is around 100 mm in the coastal areas. In the Al Hajar Mountains rainfall ranges between 100 and 350 mm. Parts of the Dhofar Mountains, influenced by monsoons, receive between 200 and 260 mm of rainfall annually. During September to November, very little precipitation is observed in the country. There are four major climatic conditions causing rainfall in Oman, which can be summarized as follows:

- Low air pressure caused by cold boundaries: it is common during winter and early spring, when it leads to rainfall fairly constant in the northern parts of the country, and scattered showers of rain in the central and southern parts of the country.
- Tropical cyclones from the Arabian Sea: the cyclones originate over the Arabian Sea and reach the Sultanate every 3 years in average in Dhofar and every 10 years in Muscat. They tend to be distributed equally between two cyclone seasons: May to June and October to November.
- Seasonal coastal currents monsoon rains: these currents are common during the period from June to September, associated with surface currents over the Arabian Sea. These currents are dominated by the south-west current, and may be mixed partly with air current coming from the Gulf of Aden. As a result, the summer in the Governorate of Dhofar is characterized by high humidity, a decrease during the months of June and July.
- Convectional rainfall: this kind of rain is the result of the presence of local convectional storms that can occur at any time during the year.

A network of 305 rain gauges covers an area of about 122,466 km^2 with daily rainfall data from 1973 to 2009. Not all of the rain gauges have records that cover the entire period from 1973 to 2009 because some gauges were dismantled, others were not accessible or damaged. It is found that by the year 2010, there were 225 rain gauges still in operation. From 1993 to 2010, a total of 115 rain gauges were operational and having common records. Considering the scarcity of data in arid regions, 17 years records are considered to be adequate for the analysis of the rain gauge network. Figure 1a shows the locations of the available rainfall data in

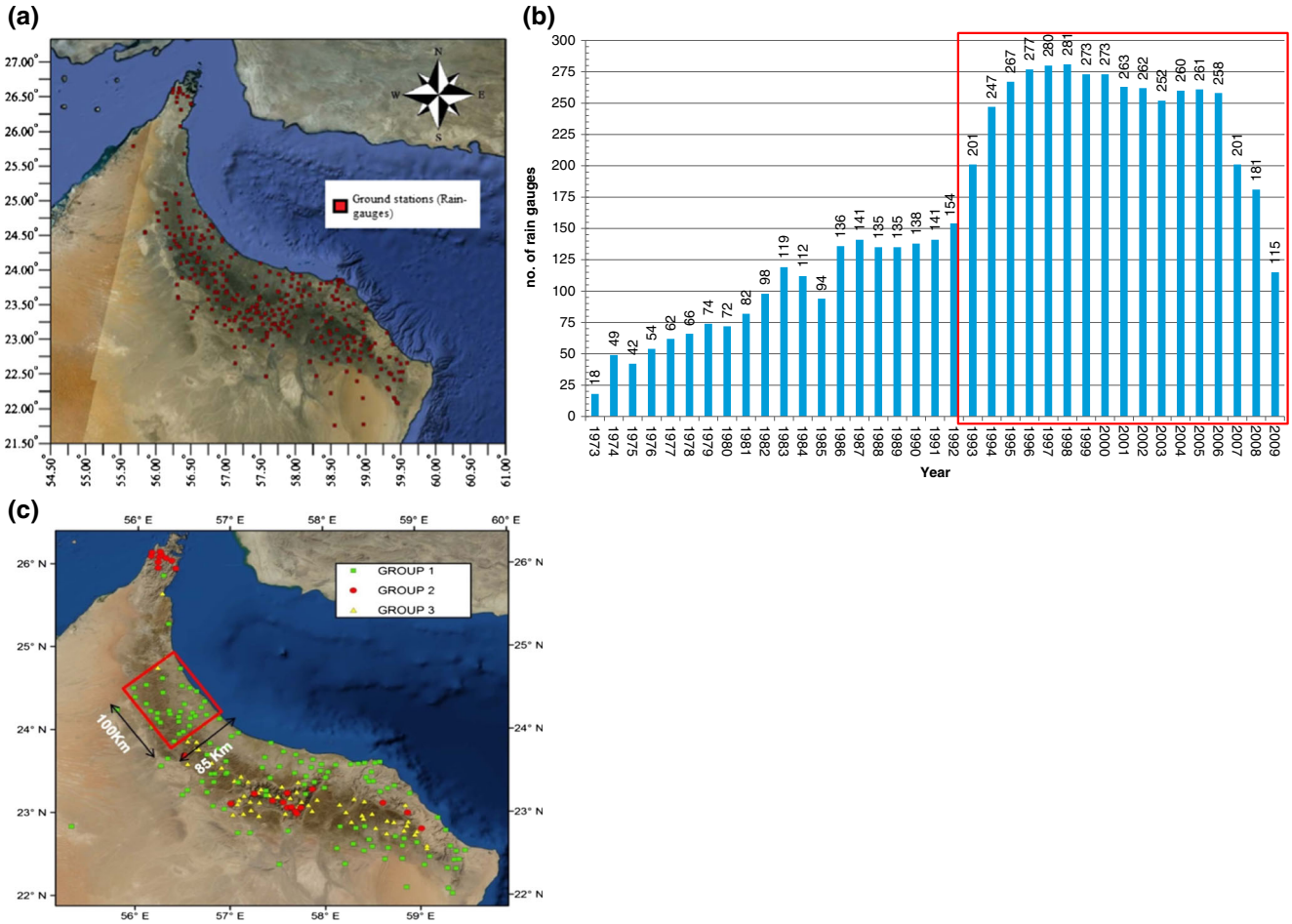

Fig. 1 **a** Area of study, Sultanate of Oman with the available ground rain gauges. **b** Number of available rain gauges (rain gauges)/year. **c** Clustering of the rain gauges in northern Oman into three clusters and the extents of the selected area of the case study in Sohar Governorate

northern Oman, Fig. 1b shows a bar chart of the number of rain gauges with records from 1973 to 2010.

The exact limit of the study area has been decided based on clustering of the rain gauges using the Agglomerative Hierarchal Clustering (AHC) dissimilarities approach. The rainfall parameters used in the clustering are the maximum daily rainfall depth and the total annual rainfall depth. Figure (1c) shows that the rain gauges are categorized into three clusters. Group 1 has an average total annual rainfall depth of 84.57 mm and an average altitude of 354.0 m above mean sea level (amsl). Group 2 has an average annual rainfall depth of 201.53 mm and an average altitude of 1219.0 m amsl. Group 3 has an average annual rainfall depth of 140.7 mm and an average altitude of 705.90 m amsl. Based on the clustering results, the selected area is located at the northern part of Oman and is entirely located in Sohar Governorate. It has a surface area of about 8500 km^2 and it includes a total of 34 rain gauges all of them belong to the clustering group 1. The selected study area extends along the coast of the Gulf of Oman from Shinas to Liwa in Sohar Governorate and extends towards the mountains up to Al Hajar Mountains to the southwest. The altitude of the area varies from +0.0 at the coastal plain to a maximum altitude of 1100.0 m amsl at the mountainous area.

Table 1 shows a summary of the different attributes of the 34 rain gauges included in the study area (rain gauge ID, easting, northing, altitude, mean annual rainfall, and maximum daily rainfall). The altitudes of the different rain gauges range from 0.7 to 832.87 amsl covering terrain conditions that extends from the coastal plains towards the Al Hajar Mountains. The mean annual rainfall ranges from 50.5 to 151.4 mm/year with the maximum value taking place at the rain gauge with the highest altitude. The maximum daily rainfall depth ranges from 42.5 to 121.8 mm/day. These attributes indicate the apparent spatial variability of the rainfall characteristics in the selected study area.

Material and methods

In this paper, the geostatistical approach of ordinary kriging is implemented using the ArcGIS Geostatistical Analyst

Table 1 Summary of the attributes of the 34 rain gauges in included in the study area in Northern Oman

(1)*	(2)**	(3)***	(4)^{x}	(5)^{xx}	(6)^{xxx}	(1)	(2)	(3)	(4)	(5)	(6)
CM996898AF	396,900	2,698,800	432.9	81.6	65.7	DM576043AF	456,679	2,670,254	201.0	55.9	60.5
CN915047AF	395,400	2,710,700	452.0	77.9	77.5	DM578762AF	459,033	2,677,420	148.6	53.1	42.5
DM089906AF	409,000	2,689,600	622.1	66.0	90.2	DM580942AF	450,426	2,689,150	168.5	73.4	74.6
DM155846AF	415,400	2,658,600	625.0	86.1	54.4	DM672387AF	462,094	2,673,060	148.9	60.4	45.0
DM173968AF	413,619	2,679,834	602.7	50.5	121.8	DM688469AF	468,551	2,684,908	44.8	52.2	48.3
DM260958BF	420,500	2,669,800	653.9	83.8	62.0	DM760001AF	470,022	2,660,114	157.8	66.0	55.0
DM264436BF	424,300	2,664,600	832.7	151.4	69.0	DM774437AF	474,272	2,674,707	69.3	61.1	85.4
DM271711BF	421,100	2,677,100	528.8	67.3	59.2	DM792227AF	472,200	2,692,700	8.8	68.6	61.6
DM339923AF	439,200	2,639,300	749.2	95.2	68.0	DM868954AF	488,500	2,669,400	13.0	73.6	70.5
DM374569AF	434,600	2,675,900	619.1	86.7	85.0	DN018590AF	408,900	2,715,000	633.7	76.2	102.0
DM383052AF	433,765	2,680,444	377.4	81.6	66.4	DN206495AF	426,924	2,704,572	527.7	63.6	56.8
DM444945AF	444,400	2,649,500	576.4	89.9	62.5	DN324310AF	426,586	2,723,896	468.2	98.2	49.8
DM459225AF	449,200	2,652,500	512.8	106.1	73.0	DN417300AF	447,523	2,713,540	69.8	63.7	80.0
DM464536AF	444,287	2,665,645	695.9	66.0	49.0	DN436617AF	446,100	2,736,700	0.7	105.0	91.0
DM474200AF	444,080	2,671,958	501.8	82.3	83.5	DN516027AF	456,200	2,710,700	9.1	91.9	103.0
DM476902AF	446,042	2,679,166	300.8	64.7	63.6	DN603661AF	463,600	2,706,100	2.3	83.7	100.3
DM565082AF	455,862	2,660,102	314.9	78.3	60.0	DM382737BF	432,300	2,687,700	528.7	79.7	68.0

*(1)** rain gauge ID, *(2)*** rain gauge easting (m), *(3)**** rain gauge northing (m), *(4)*^{x} rain gauge altitude (amsl), *(5)*^{xx} mean annual rainfall (mm/year), and *(6)*^{xxx} maximum daily rainfall (mm/day)

extension to evaluate the performance of the existing rain gauge network in the study area and to propose any necessary augmentation of the network. The following sub-sections present the approach and methodology that we adopted to achieve the objectives.

Rainfall interpolation using geostatistical approach

Spatial interpolation is commonly performed by guessing a regionalized value at un-gauged locations using the weights of other observed regionalized values. In this paper, un-gauged points refer to the centers of a rectangular mesh of 1-km^2 covering the selected study area. The general equation for spatial interpolation is given by Eq. (1) as follows:

$$Z_g = \sum_{i=1}^{i=N} \varphi_i Z s_i \quad (1)$$

where Z_g is the interpolated value at point g, Zs_i is the observed value at point i, N is the total number of observed rain gauges, and φ_i is the individual weight of each rain gauge contributing to the interpolation. The focus of the interpolation procedure is the accurate calculation of the individual weight contribution φ_i at other points. The literature include different approaches frequently practiced for calculating these weights, e.g., Thiessen polygon method (Chow 1964), inverse distance weighting method (Teegavarapu and Chandramouli 2005), and the geostatistical methods.

Geostatistical approaches have been applied in the interpolation and evaluation of any monitoring networks including rain gauge networks. The geostatistical approaches produce un-biased interpolated estimates with minimum variance error. The semivariograms are the main tools used in geostatistical approaches to characterize the spatial variation and spatial dependence in the rainfall distribution. By using Kriging, the best linear un-biased estimate of the interpolated value can be estimated at each location. Kriging usually employs a theoretical semivariogram model to represent the spatial dependence between the different observed points. An empirical semivariogram is initially developed using the observed records from the different rain gauges and hence used in the development and evaluation of the appropriate theoretical semivariogram. Different forms of Kriging are reported in the literature, ordinary Kriging (Ly et al. 2011), universal Kriging (Basistha et al. 2008), kriging with an external drift (deutsch 1996), and ordinary cokriging (Goovaerts 2000) are the most common kriging methods.

Ordinary kriging is one of the most widely used geostatistical methods due to its computational simplicity and data availability in different applications. The optimal interpolation in Kriging is based on regression against observed rainfall Zs_i which is a random variable defined at location s_i and it is assumed to be a second-order stationary random field. To estimate the unknown value of Z_g at an ungauged location, the general formula of the interpolated value is given by Eq. (1). The weights φ_i are obtained using the semivariogram model such that the weights are not biased

and the variance is minimized. The ordinary Kriging equations set of ($ns + 1$) is given by Eq. (2) as follows:

$$\sum_{i=1}^{ns} \varphi_i \gamma_{ij} - \mu = \gamma_{i0} \qquad for\ j = 1, \ldots, ns \tag{2a}$$

$$\sum_{i=1}^{ns} \varphi_i = 1 \tag{2b}$$

where γ_{ij} represents the calculated semivariances of Zs_i between any two locations i and j, and μ is the Lagrange parameter. The weights φ_i that will be derived from Eq. (2) will feed Eq. (1) in order to get the interpolated values of the variables. To avoid biased predictions, the summations of the weights of φ_i are forced to be 1, which necessitates the identification of the Lagrange parameter.

Semivariogram modeling

The random nature of spatial variation of rainfall phenomena can be represented by a random field $Z(x)$, where x represents the spatial location and Z is the rainfall depth. The distance separating between pair of rain gauges is known as the lag vector (h). $z(u)$ represents the rainfall depth as a function of spatial location and $z(u + h)$ represents the lagged version of the rainfall depth as a function of spatial location. As we can think of the two variables as located at the tail and head of the lag vector, the $z(u)$ can be referred to as the tail variable and the $z(u + h)$ can be referred to as the head variable. The spatial variation structure of the rainfall depth $Z(x)$ with a stationary mean can be represented by its semivariogram, defined by Eq. (3):

$$\text{Semivariance} : \gamma(h) = \frac{1}{2N(h)} \sum_{\alpha=1}^{N(h)} [z(u_\alpha + h) - z(u_\alpha)]^2 \tag{3}$$

where $N(h)$ is the number of data pairs separated by lag distance plus or minus the lag tolerance, and the $\gamma(h)$ is the semivariance. The semivariance is the moment of inertia or spread of the scattergram about the 45 degrees line. Unlike the correlation and covariance which are measures of data similarity, the semivariance is a measure of data dissimilarity.

Equation (3) shows that the semivariance is independent of the locations of different points, i.e., it only depends on the distance between the two points under consideration. The plot of the semivariance versus the lag is called the semivariogram. The influence range of a semivariogram is the minimum distance $|(u + h) - (u)|$ beyond which the random variables observed at two points separated by a lag distance, $z(u + h)$ and $z(u)$, become independent. For a second-order stationary random field, as the lag distance h increases, the semivariance will reach an asymptotic value, known as the sill, denoted by c, which is numerically the same as the variance of the random variable $z(u)$. Theoretically, the semivariogram value at the origin should be zero; however, if it significantly deviates from zero at very small lag distances, then the semivariogram value at the origin is called nugget. The nugget represents the spatial variability at small lag distances that are less than the sampling distance or represents measurements errors. For further details of semivariogram modeling, refer to Bohling (2005) and Adhikary et al. (2015b).

After developing the empirical semivariogram derived using the observed data, the theoretical semivariogram model should be identified. This theoretical model is necessary because the ordinary kriging algorithm needs to get the semivariance values for other lag distances rather than those used in the development of the empirical semivariogram. Also, to ensure solvable ordinary kriging equations, the selected semivariogram model needs to conform certain numerical properties. Two of the most commonly used basic theoretical semivariogram models are applied herein. These are the spherical model (Eq. 4) and the exponential model (Eq. 5). Each of these models is combined with a nugget effect.

$$\text{spherical semivariogram model} : g(h) = \begin{cases} c.\left(1.5\left(\frac{h}{a}\right) - 0.5\left(\frac{h}{a}\right)^3\right) & \text{if } h \le a \\ c & \text{otherwise} \end{cases} \tag{4}$$

$$\text{Exponential semivariogram model} : g(h) = c.\left[1 - \exp\left(\frac{-3h}{a}\right)\right] \tag{5}$$

Whereas $g(h)$ represents the semivariance for a pair of data points separated by a lag distance h. c is the asymptotic maximum value of the semivariance, and a is the range or the distance at which the random variables become independent. The spherical model reaches the specified sill value, c, at the specified range, a. The exponential model approaches the sill asymptotically, with a representing practical range which is the distance at which the semivariance reaches 95 % of the sill value.

Evaluation criteria of the interpolation

The evaluation of the kriging interpolation using different semivariogram models is carried out using cross-validation. This process involves temporarily discarding data from the sample dataset and then estimating such values using the remaining samples (Isaaks and Srivastava 1989). In this way, the predicted values can be compared with the observed values at the same location and consequently get useful information about the kriging model and how good it works.

Summary statistics are made by comparing the predicted value to the actual value from cross-validation given that Zs_i is the predicted value from cross-validation, Zg_i is the observed value and σs_i is the predication standard error for location s_i. Johnston et al. (2001) provided five summary statistics for

evaluating geostatistical models. These are mean prediction error (Eq. 6), root mean square prediction error (Eq. 7), average kriging standard error (Eq. 8), mean standardized prediction errors (Eq. 9), and root mean square standardized prediction error (Eq. 10).

$$\text{Mean prediction error} = \frac{\sum_{i=1}^{n}(Zs_i - Zg_i)}{n} \tag{6}$$

Root mean square prediction error

$$= \sqrt{\frac{1}{n}\sum_{i=1}^{n}(Zs_i - Zg_i)^2} \tag{7}$$

$$\text{Average kriging standard error} = \sqrt{\frac{1}{n}\sum_{i=1}^{n}\sigma s_i} \tag{8}$$

Mean standardized prediction error

$$= \frac{\sum_{i=1}^{n}(Zs - Zg_i)/\sigma s_i}{n} \tag{9}$$

Root mean square standardized prediction error

$$= \sqrt{\frac{1}{n}\sum_{i=1}^{n}((Zs_i - Zg_i)/\sigma s_i)^2} \tag{10}$$

The mean prediction error is used to assess the degree of bias in the predictions. For un-biased predictions, the mean prediction error should be near zero. The mean standardized prediction error is estimated by dividing the mean prediction errors by the prediction standard error. For un-biased predictions, the mean of the standardized prediction error should be also near to zero. To have the predictions as close to the observed values as possible, the root mean square prediction error is computed, the closer the predictions are to the observations, the smaller will be the root mean square prediction error. The standardized root mean square error shall be near to or equal to 1.0 to have a model that neither overestimates nor underestimates the variability in the predictions.

Characterization of the acceptable accuracy

Cheng et al. (2008), Kassim and Kottegoda (1991), and Bastin et al. (1984) used the ordinary kriging variance for optimal estimation of areal rainfall average using an interactive selection procedure. The ordinary Kriging estimation variance is given by Eq. (11) as follows.

$$\sigma_k^2(x_0) = \mu + \sum_{i=1}^{ns}\varphi_i\gamma_{i0} \tag{11}$$

A reliable rain gauge network should have an acceptable accuracy of rainfall estimation at most of the points within the area served by the network. The estimate rainfall at any point can be considered acceptable if it falls within a certain range of the actual value. By taking into account that the estimation accuracy of rainfall varies from time to time and from one event to another and taking into consideration the variance of the rainfall field, the formula of the probability of acceptance provided by Cheng et al. (2008) is used, Eq. 12.

$$P\left[\left|Z_g(x_0) - Z_g(x_0)\right| < k\sigma_k\right] \le a \tag{12}$$

where $Z_g(x_0)$ is the true rainfall at a certain location (x_0) and $Z_g(x_0)$ is the kriging estimation of the rainfall at the same location, k is a multiple and a is the minimum acceptance probability selected on the basis of the factors such like available budget for gauge installation, maintenance level, and required estimation accuracy. We calculated the provability of acceptance for two thresholds of acceptance (a = 0.85 and 0.9). The percentage of the area that achieves the minimum acceptance probability (A_p) is calculated and used as basis for rain gauge network evaluation.

Evaluation of the existing rain gauge network

The percentage of area with acceptable accuracy is used as the basis for rain gauge network evaluation. On the same basis, rain gauge network augmentation can be achieved by adding new rain gauge or removing/relocating existing rain gauges. In order to enable the augmentation process, exiting rain gauge is ranked and prioritized. Ranking will identify the base rain gauges which are essential in the network and cannot be removed or relocated and the non-base gauges which are subject to removal or relocation to new sites.

A sequential ranking algorithm suggested by Cheng et al. (2008) is applied to rank and prioritize rain gages in the existing network. In this algorithm, one gauge at a random location, hereafter referred to as gauge, is chosen from a set of m remaining rain gauges. The algorithm starts with a set of remaining rain gauges consisting of all existing rain gauges. At each grid node, the variance of the estimation error is calculated using Eq. (11) with only rain gauges involved. Then, the area of acceptable accuracy with the remaining gauges in place is calculated. The next step will be to return the previously selected rain gauge to the set of existing rain gauges (m) and to select a different rain gauge and recalculate the variance of the estimation error and the area of acceptable accuracy for the remaining rain gauges. This process is repeated until all rain gauges in the network are selected and the areas of acceptable accuracy are calculated in each step. The rain gauges are then ranked according to their corresponding areas of acceptable accuracy. The rain gauge with the highest area of acceptable accuracy is the least important gauge with no significant contribution to the area of the acceptable accuracy provided by the network, i.e., with no added value to the areal estimation of rainfall. This gauge is then removed from the network and the whole above-mentioned procedure is repeated again on the remaining rain gauges. This algorithm is repeated until there is only one rain gauge remaining.

Results and discussion

Exploratory Analysis of the observed rainfall data

Geostatistical methods are optimal when the input data are normally distributed and spatially stationary, i.e. the mean and variance of the data does not vary significantly in space. Significant deviations from normality and stationary may lead to violation of the method assumptions. As such, the analysis begins by looking at a histogram plot to check for normality and plotting of the data values in space to check for significant trends.

Figure 2a shows the distribution of the average mean annual rainfall data for the 35 rain gauges included in the case study. The distribution indicates a skewness coefficient of 1.5611 and a kurtosis coefficient of about 7. According to this, the original mean rainfall data cannot be considered as normally distributed and shall be subject to transformation prior to the application of further analysis. The appropriate method used for transformation in this case is the Box-Cox transformation. Figure 2b shows the distribution of data after being transformed using the Box-Cox, with a transformation parameter of −0.8. The transformed data resulted in a skewness coefficient of −0.03182 (nearly equal to zero) and a kurtosis coefficient of 2.888 which can be considered as normally distributed data.

For a second order stationary rainfall depth, the semivariogram approaches its sill, which numerically equals to the variance of the rainfall. The existence of an orographic or spatial trend in the data will eliminate the condition of second-order stationarity and causes the semivariogram to increase continuously without a sill. Therefore, it is necessary to explore the orographic and spatial trend in the observed rainfall data prior to fitting a semivariogram model.

The spatial trend is explored by plotting the values of the mean annual rainfall data of all rain gauges over X–Y plane with Z-axis representing the rainfall depth at each rain gauge. A second-order polynomial is fitted to the rainfall data on both north-south and east-west directions. Figure 3 shows that a clear orographic trend exists in the east-west direction. In the east-west direction of the study area, there is the coastal plain followed by Al Hajar Mountains and then followed by the inland plains. The rainfall records are highest over the mountainous zone compared to the plains because of the orographic effect. It is worth noting that since the data have a trend effect in both directions; it may also be subject to anisotropy. This will be subject to further checking while executing the semivariogram fitting. De-trending is applied to the data in order to remove the existing trend by subtracting the trend surface (second-order polynomial function). The residuals, after the de-trending are used in fitting the semivariogram model. In the kriging process, the global trend is added back

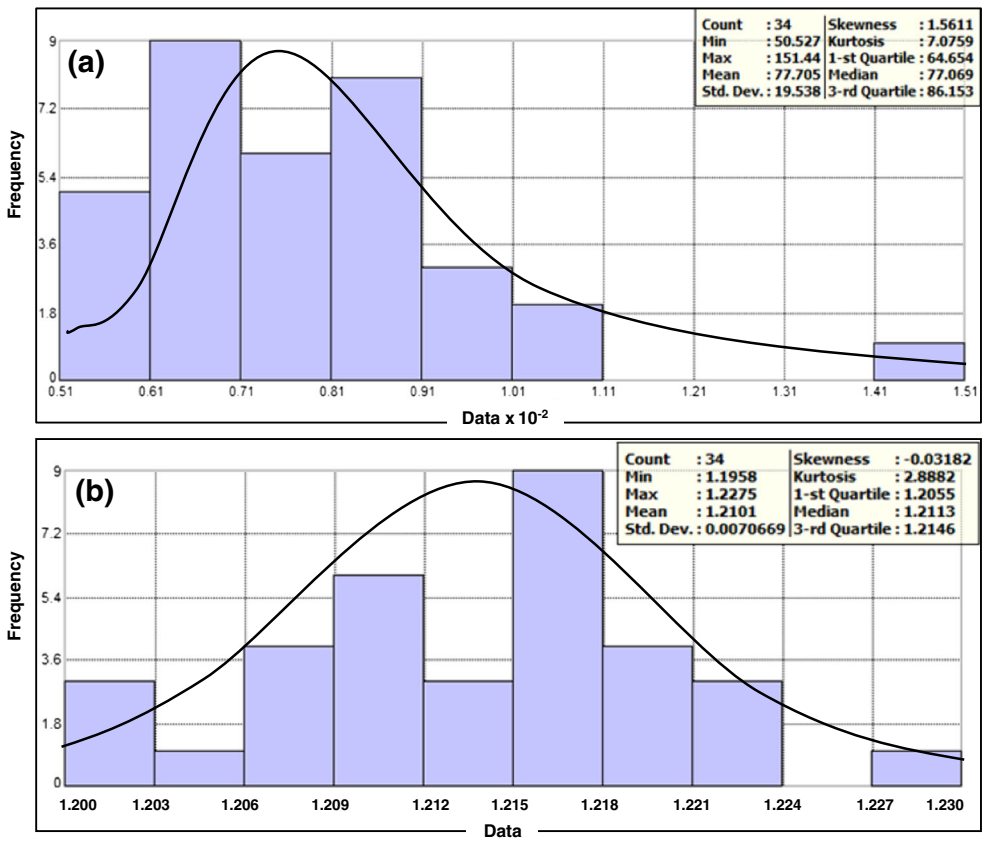

Fig. 2 Histogram distribution of the mean annual rainfall data **a** before transformation and **b** after transformation

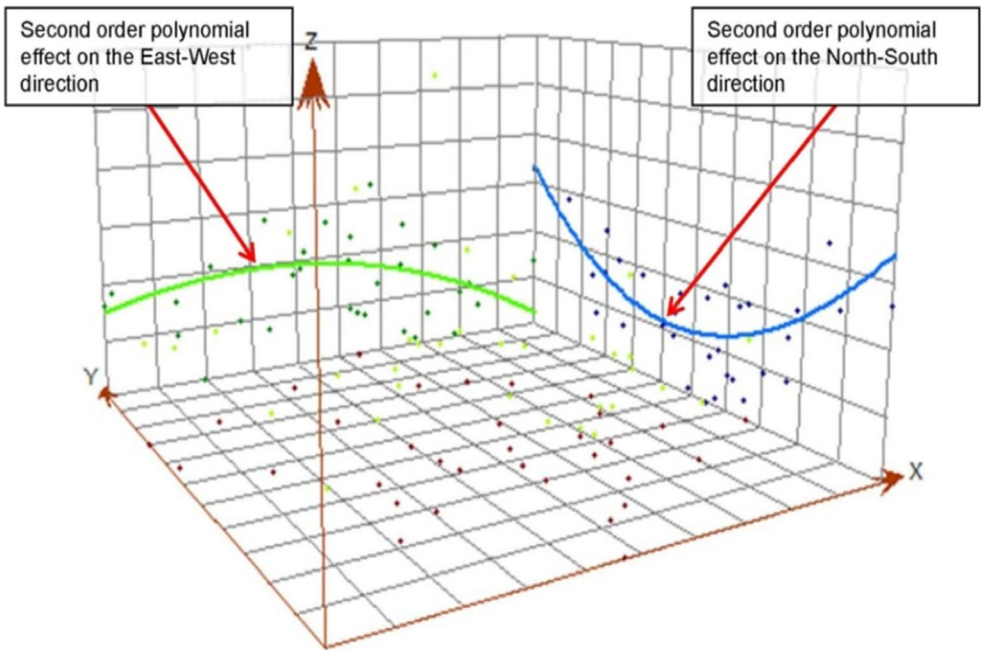

Fig. 3 Spatial trend of the mean annual rainfall data records for different rain gauges in the study area in different directions

to the data such that the kriging interpolation is carried out on the original mean rainfall data.

Fitting of semivariogram model

The spherical and exponential semivariogram models are both fitted to the de-trended mean annual rainfall data. Figure 4 shows the resultant semivariograms for the exponential model (Fig. 4a) and the spherical model (Fig. 4b). As we are working in a two dimensional space, it is expected that the semivariogram and covariance functions may not only change with distance, but also with direction (anisotropy). The check for the spatial trend shown in Fig. 3 illustrated second order polynomial trends on north-south and east-west directions which favor the case of anisotropy. Anisotropy can be explained by prevailing wind direction, orography, etc. By checking the semivariogram cloud in several directions, it is evident that the semivariance of the mean annual rainfall depth varies not only with distance but also with direction for the same lag distance. As such the space can be considered under anisotropy effect. Figure 4 shows the relation between the de-trended semivariance values on the vertical axis and the lag distance on the horizontal axis for all pairs of stations. Each line inside the envelop represents the best fit model in a specific direction. Based on the generated best fit models, the major and the minor ranges as well as the angle of influence are calculated.

Figure 5 shows the directional anisotropy of the exponential semivariogram model. The model resulted in a prevailing directional anisotropy at 30.0° from the north with a major range between pairs of rain-gauges of 33663.20 m. The minor range in the perpendicular direction (120.00°) equals 18655.10 m. The spherical model resulted in an angle of directional anisotropy of 33.40°, a major range of 33972.50 m, and a minor range of 21445.40 m (results are not shown). This indicates that both models reached the same sill value at similar values for the major and minor ranges. It is also noted that the directions of anisotropy are

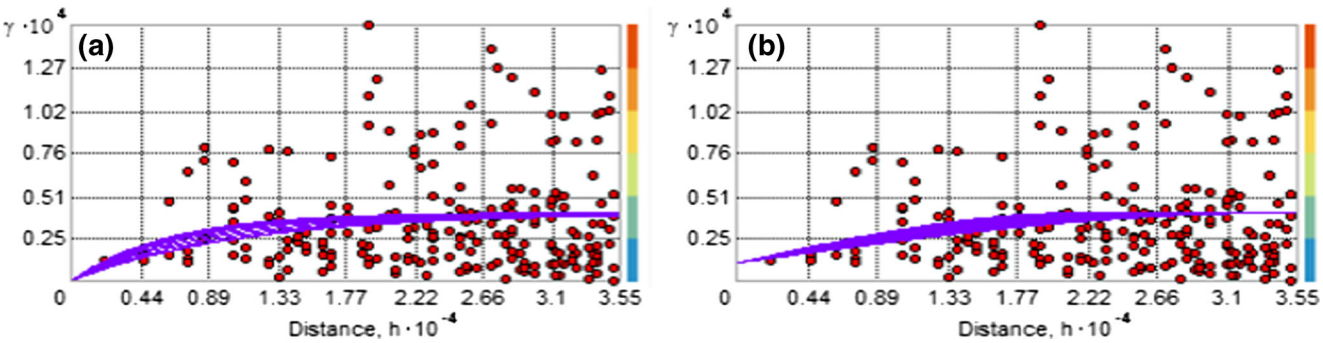

Fig. 4 Anisotropy semivariogram model envelop. Exponential model on the average of total annual rainfall

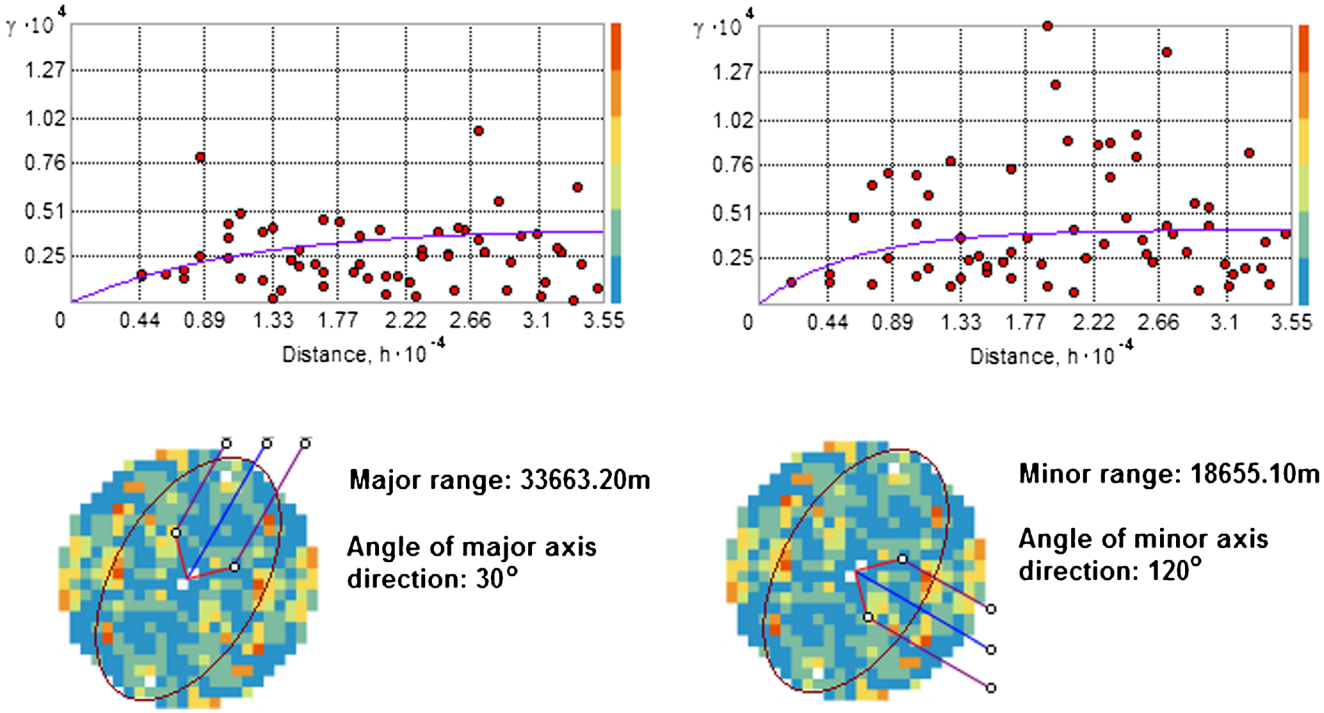

Fig. 5 Check of directional anisotropy for the exponential semivariogram model for the mean annual rainfall data

also close to each other. This is logical since the anisotropy is not directly related to the theoretical model to be fitted, but it is more relevant to geography and wind directions, etc.

Applying kriging interpolation

The weights for the kriging interpolation are acquired using the surrounding measured values to predict values at each

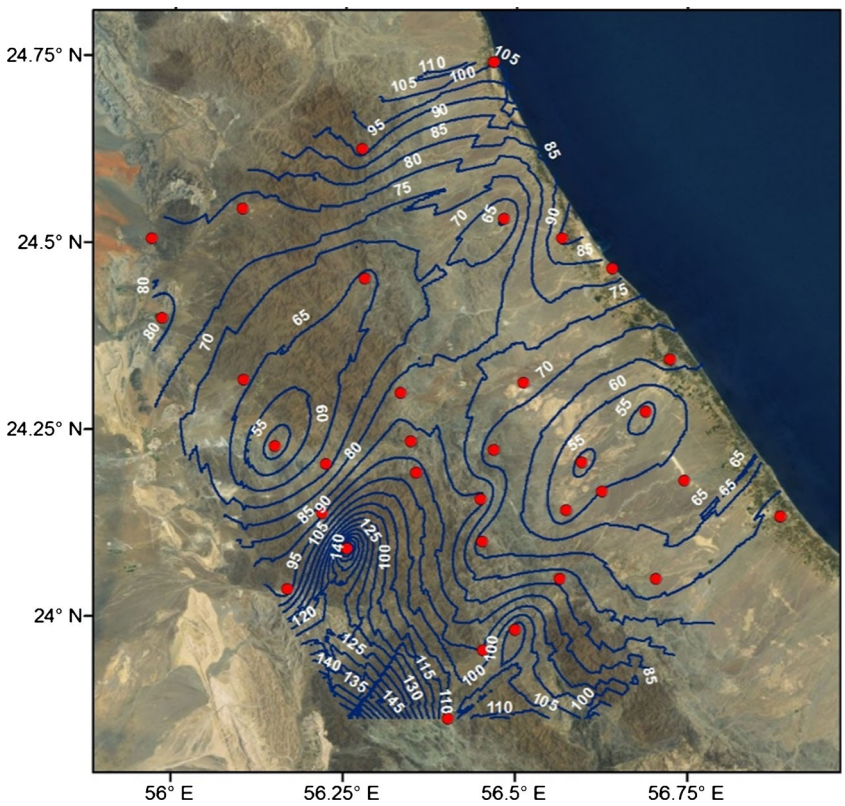

Fig. 6 Interpolated annual mean rainfall of the study area using ordinary Kriging based on exponential semivariogram model

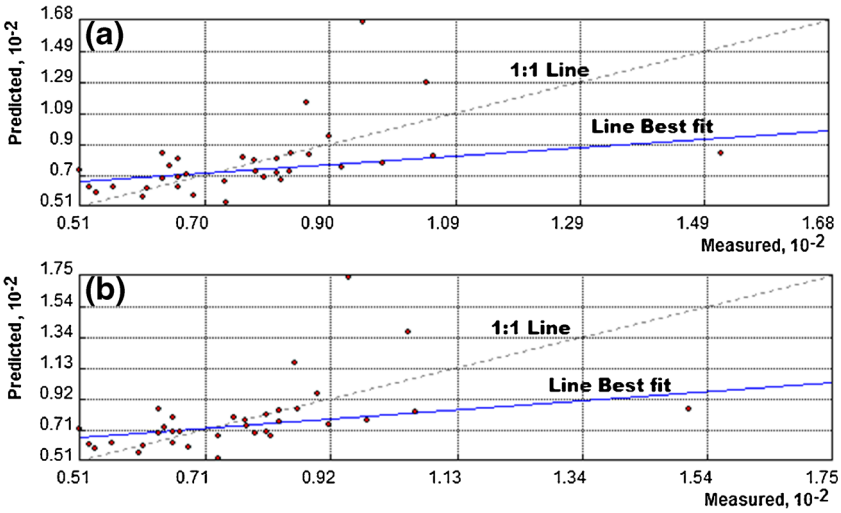

Fig. 7 Cross-validation scatter plot of the mean annual rainfall depth, **a** spherical semivariogram and **b** exponential semivariogram model

point in a mesh that consists of 1-km grid points. The kriging weights come from the theoretical semivariograms that was developed by looking at the spatial structure of the data. The interpolated rainfall at each grid point is estimated based on the semivariogram and the spatial arrangement of nearby observed values. The contours of the interpolated mean annual rainfall generated by ordinary Kriging based on the exponential semivariogram model are shown in Fig. 6. The mean annual mean rainfall varies from 55 to 150 mm/year, with an aerial mean of 85 mm/year.

Statistical measures are used to evaluate the interpolated rainfall acquired using the exponential and the spherical semivariogram models. Figure 7 shows the cross-validation values of the interpolated de-trended mean annual rainfall versus the observed values acquired using the exponential semivariogram model (Fig. 7a) and using the spherical semivariogram model (Fig. 7b).

Table 2 summarizes the statistical measures (i.e., mean prediction error, mean prediction standardized error, average kriging standard error, root mean square prediction error, and standardized root mean square prediction error). For both models, the statistics indicate that the mean prediction error and the mean standardized prediction error for both semivariogram models are close to zero. In addition, the root-mean square standardized prediction error is close to 1.0, which give a good indication that unbiased predictions are reached and that the two semivarigram models neither overestimates nor underestimates the observations. Accordingly, the used criteria have adequate estimation of the areal mean annual rainfall over the study area. It is noted that there is no significant difference between the two semivarigram models and both are representative of the spatial variability in the annual rainfall in the study area. Hence, it is decided to select the exponential model for further analysis.

Network performance evaluation

This step is the main goal of the previously explained geostatistical analysis. The rainfall estimation accuracy at each grid point can be evaluated using the acceptance probability. The performance evaluation of the rain gauge network has been made based on the area with acceptance probability, hereinafter expressed by A_p. A_p is calculated at each point in the study area after being discretized into a grid of 1-km mesh size which enables the establishment of contour maps for the acceptance probability.

Figure 8 shows contour maps of acceptance probability for the mean annual rainfall over the study area. Figure 9 shows the area of acceptable accuracy (A_p) of the mean annual rainfall depth for of 0.90 (Fig. 9a), and for of 0.85 (Fig. 9b). At α

Table 2 Statistical measures of the goodness of the exponential and spherical semivariogram models

Semivariogram model	Mean prediction error (Eq. 6)	Root mean square prediction error (Eq. 7)	Average kriging standard error (Eq. 8)	Mean standardized prediction error (Eq. 9)	Root mean square standardized prediction error (Eq. 10)
Exponential semivariogram	0.70	21.25	18.77	−0.024	1.01
Spherical semivariogram	0.90	21.99	18.91	−0.108	1.23

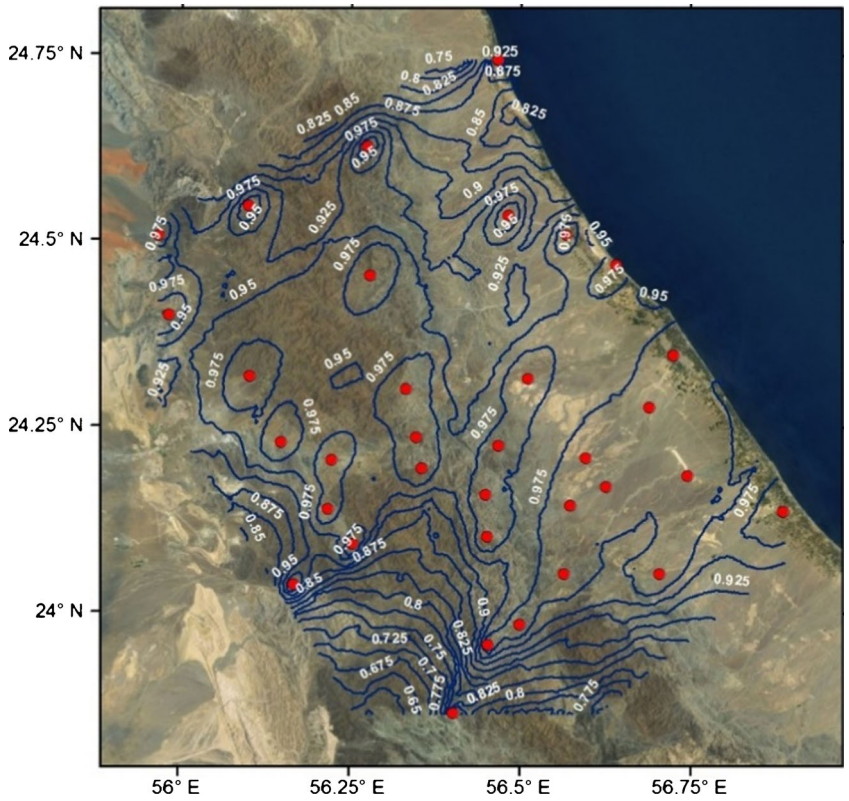

Fig. 8 Contours of acceptable probability for the mean annual rainfall depth

= 0.90, the area of acceptable accuracy $A_p \approx 77.72$ % of the total study area. The remaining 22.28 % of the area, shaded in grey, did not achieve the predetermined level of acceptance. It means that the existing rainfall network could not provide adequate spatial coverage for predicting the mean annual rainfall at 22.28 % of the study area. With a relaxed and less conservative acceptance threshold with set to 0.85, the area of acceptable accuracy increased to 88.71 % and the remaining 11.29 % of the area did not achieve the success threshold. In the vicinity of the rain gauges, the acceptance probability is close to 1.0 and it decreases as we are going far from the rain gauges. This is because the ordinary kriging interpolation results are exact rainfall predictions at the locations of the rain gauges with zero kriging estimation error.

The decision of whether the performance of the existing rainfall network is acceptable or it needs further augmentation depends on a pre-determined threshold of the area of acceptable accuracy. If the authorities set as an acceptance threshold,

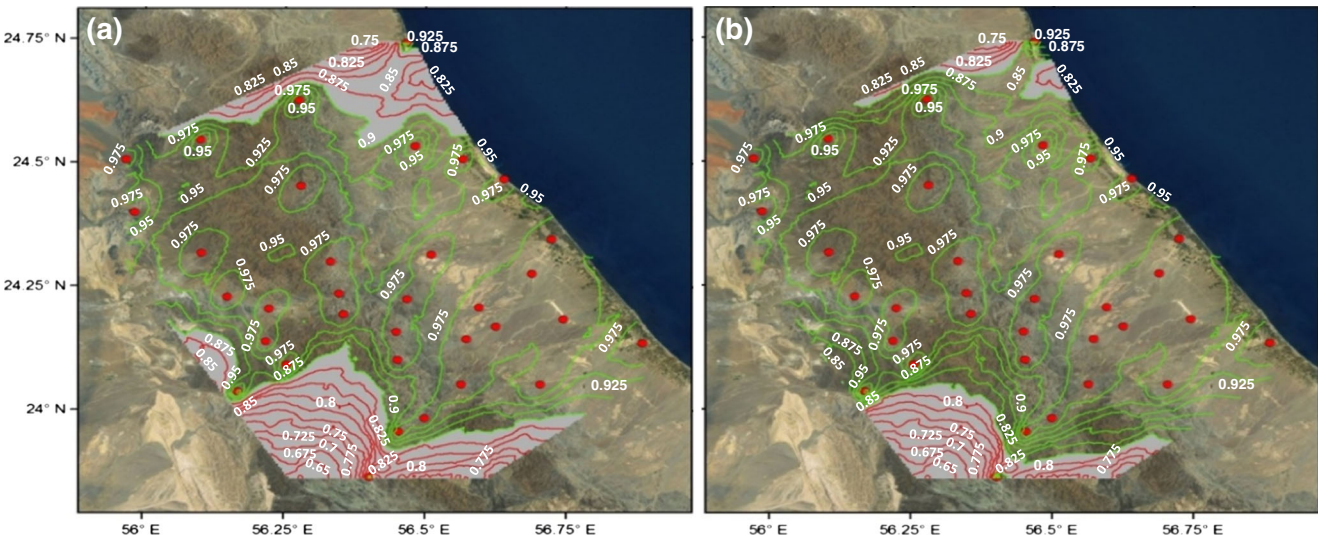

Fig. 9 Area of acceptable accuracy (A_p) of mean annual rainfall depth for **a** $a = 0.90$ and **b** $a = 0.85$

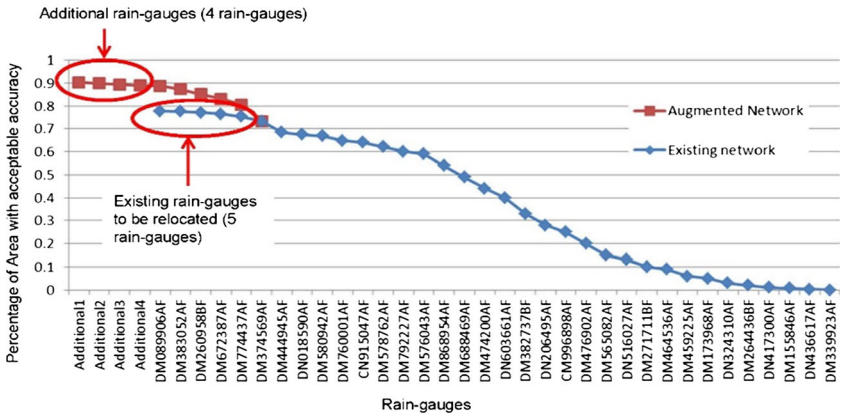

Fig. 10 Prioritization of the 34 rain gauges. Mean annual rainfall data and effect of relocation/ addition of rain gauges

that 80 % of the area should be with acceptable accuracy limits, then the existing rain gauge network would pass the criterion for set to 0.85 and it will not meet the criterion for set to 0.90. The area of acceptable accuracy for set to 0.85 is 88.71 % indicating a pass result and the area of acceptable accuracy for set to 0.9 is 77.72 % indicating the need for augmentation. The value of and the threshold of the area of acceptable accuracy depend on the purpose of the network, the downstream uses of the data, as well as on the economic constraints, budget availability, and authorities' willingness to upgrade the existing rain gauge network.

Prioritization of rain gauges and augmentation of the existing network

It is important to prioritize the rain gauges within the study area to have an idea about the rain gauges essential to keep and the other less important gauges (non-base gauges).The base gauges be kept in their location and the non-base gauges can be stopped or relocated in order to improve the area of acceptable accuracy. The sequential algorithm, described in the methodology, is applied to the existing rain gauge network to carry out the network augmentation.

Figure 10 shows the 33 steps carried out for prioritizing the rain gauges with their corresponding areas of acceptable accuracy. According to the prioritization, rain gauges number DM089906AF, DM383052AF, DM260958BF and DM672387AF didn't significantly increase the area of acceptable accuracy. Accordingly, these rain gauges can be stopped to reduce the cost of operation and maintenance or they can be relocated to increase the percentage of area with acceptable accuracy. The remaining 29 rain gauges that were not removed or relocated form the base rain gauges in the network.

We also considered providing additional rain gauges in addition to relocating the above-mentioned rain gauges. New rain gauges are added in locations where the area of acceptable accuracy is less than 0.85 (shaded area in Fig. 9). In order to perform this, the predicted value from the kriging interpolation at the ungauged locations is used as input to the augmented rain gauges configuration. The area of acceptable accuracy is recalculated for the new set of rain gauges in the network to determine the added

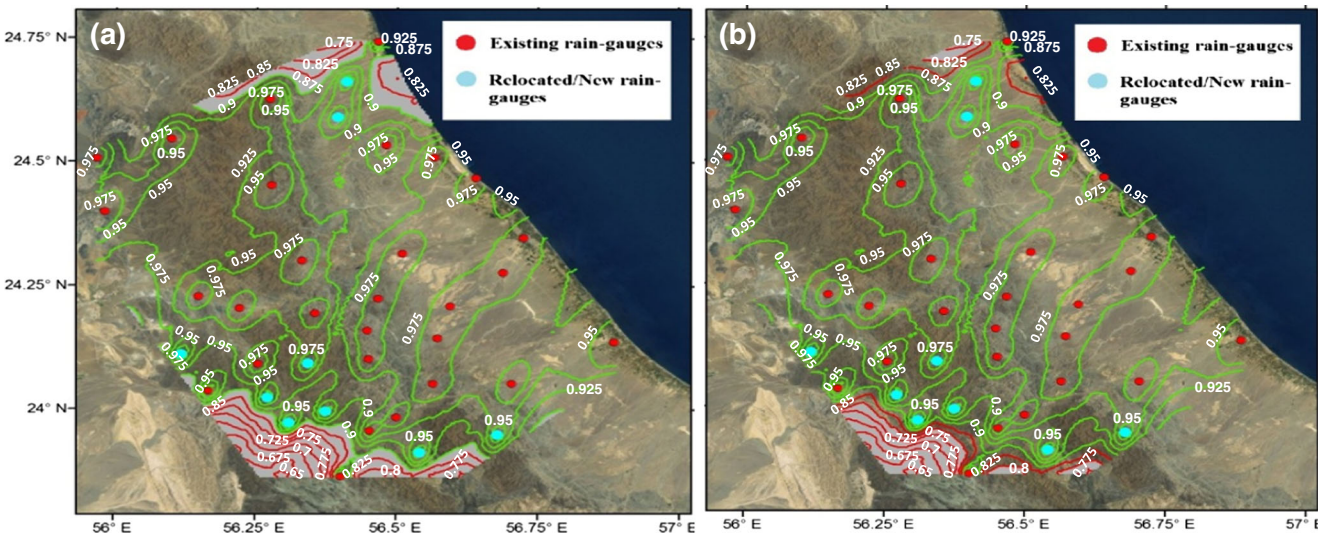

Fig. 11 Area of acceptable accuracy after augmentation for the mean annual rainfall **a** for $\alpha = 0.90$ and **b** for $\alpha = 0.0.85$

value from network augmentation, i.e., after adding new rain gauge and relocating other rain gauges.

Figure 11 shows the area of acceptable accuracy for the predicted mean annual rainfall after relocating the above mentioned 5 rain gauges and adding new 4 rain gauges. Figure11 considers both acceptable accuracy thresholds of α=0.90 and α=0.85. The rain gauges in red color are the existing rain gauges and those in cyan are both the relocated/additional rain gauges. From the new configuration, it is found that the area of acceptable accuracy for the average total annual rainfall data increased from 77.72 % to 90.50 % for acceptable accuracy threshold of α=0.90 and from 88.71 % to 94.51 % for acceptable accuracy threshold of α=0.85.

Conclusions

A geostatistical approach for evaluation and augmentation of an existing rain gauge network is presented. The evaluation approach is based on estimating the total area that achieves the targeted level of acceptable accuracy. The variances of estimation error at un-gauged locations were calculated using ordinary kriging approach and were assumed to be normally distributed. The acceptance probabilities were defined as the kriging estimation error falls within a predetermined range of standard deviation of rainfall. Kriging estimation errors with probability of acceptance that equals to or exceeds a given threshold value of α = 0.85 or 0.90 are assumed to have acceptable accuracies. A predetermined value of the total area that satisfied the above criterion is set as a limit for evaluation and need for augmentation of the exiting network. A sequential algorithm is also applied to prioritize the existing rain gauges, identify the base rain gauge in the network and to provide recommendation for omission and relocation of other non-base gauges.

A study area in northern Oman located in Sohar governorate is selected as a pilot case. The area has 34 rain gauges and it is characterized by a terrain surface that varies from coastal plain to mountains. The mean annual rainfall exhibited significant orographic effects due to the prevailing terrain conditions. For a threshold value of acceptance probability of 0.85, the existing network achieved 88.71 % of the total area with acceptable accuracy for mean annual rainfall data. Also for a threshold value of acceptance probability of 0.90, the existing network achieved 77.72 % of the total area with acceptable accuracy for mean annual rainfall data. For a success criterion of 80 %, the existing rain gauge network indicates acceptable performance for acceptance probability threshold of 0.85. However, inadequate performance is noticed in the case of probability threshold of 0.90 which necessitated further network augmentation.

Using a sequential algorithm for ranking and prioritization of the existing rain gauges, all rain gauges were classified into base and non-base rain gauges. The base rain gauge network for mean annual rainfall comprised about 29 of the existing rain gauges. The base rain gauge network can achieve almost the same level of the percentage of area with acceptable accuracy as the complete network that consists of 34 gauges. The identified non-base rain gauges were sequentially relocated to achieve higher levels of percentage of area with acceptable accuracy. For the mean annual rainfall data, the percentage of area with acceptable accuracy increased from 88.71 % for the original rain gauge network to about 94.51 % for the augmented network by adding four rain gages at a probability acceptance threshold of 0.85. It also increased from 77.72 % for the existing network to 90.50 % for the augmented rain gauge network at an acceptance threshold of 0.9.

The presented approach focused on estimating the accuracy of areal rainfall across the study area. It is more convenient to be applied in catchments with high-intensity rainfall and short time of concentration. The approach is flexible in regards to the parameters used in accuracy assessment such as the threshold of the probability of acceptance and criterion for the percentage of area with acceptable accuracy. The previous analysis could be reapplied in the evaluation of the same rain gauge network but based on higher temporal resolution rainfall data (e.g., maximum daily rainfall). This will be useful in examining the performance of the existing rain gauges in applications related to storm water management and flood protection.

Finally, we conclude that the commonly used WMO recommendations shall not be considered as a general governing rule for the minimum number of rain gauges applicable anywhere. One must take into consideration that the rain gauge network must be able to reproduce the spatial rainfall pattern in the area. It is not only the density of rain gauges that govern the performance of the network, but also the exact location of rain gauges in a crucial factor.

Acknowledgments Acknowledgments are due to Dar Al Handasah, Shair and partners for providing the needed software tools logistical support to the authors during the study. Special thanks to Prof. Alaa Alzawahry from Cairo University, Egypt, for his guidance and support provided through the study. The authors are grateful to the Ministry of Regional Municipalities and Water Resources in the Sultanate of Oman for providing the rainfall records for the case study. Finally, authors would like to express their gratitude and thanks to the anonymous reviewer and editor for their comments and suggestions that significantly enhanced the quality of the paper.

References

Adhikary SK, Abdullah GY, Nitin M (2015a) Optimal design of rain gauge network in the Middle Yarra River catchment, Australia. Hydrol Process 29(11):2582–2599. doi:10.1002/hyp.10389

Adhikary SK, Muttil N, Yilmaz AG (2015b) Genetic programming-based ordinary kriging for spatial interpolation of rainfall. J Hydraul Eng ASCE 21(2). doi:10.1061/(ASCE)HE.1943–5584.0001300

Ali A, Lebel T, Amani A (2005) Rainfall estimation in the Sahel. Part I: error function. J Appl Meteorol 44:1691–1706. doi:10.1175/JAM2304.1

Basistha A, Arya DS, Goel NK (2008) Spatial distribution of rainfall in Indian Himalayas—a case study of Uttarakhand Region. Water Resour Manag 22(10):1325–1346

Bastin G, Lorent B, Duque C, Gevers M (1984) Optimal estimation of the average areal rainfall and optimal selection of rain gauge locations. Water Resour Res 20(4):463–470. doi:10.1029/WR020i004p00463

Bohling G (2005) Introduction to geostatistics and variogram analysis. http://people.ku.edu/~gbohling/cpe940/Variograms.pdf. Accessed 5 May 2016

Carrera-Hernandez JJ, Gaskin SJ (2007) Spatio temporal analysis of daily precipitation and temperature in the basin of Mexico. J Hydrol 336(3):231–249. doi:10.1016/j.jhydrol.2006.12.021

Chebbi A, Zoubeida KB, Maria da Conceição C (2011) Optimal extension of rain gauge monitoring network for rainfall intensity and Erosivity index interpolation. J Hydrol Eng 16(8):665665–665676. doi:10.1061/(ASCE)HE.1943-5584.0000353

Chen YC, Chiang W, Hui-Chung Y (2006) Rainfall network design using kriging and entropy. Hydrol Process 22(3):340–346. doi:10.1002/hyp.6292

Cheng KS, Lin YC, Liou JJ (2008) Rain-gauge network evaluation and augmentation using geostatistics. Hydrol Process 22(14):2554–2564. doi:10.1002/hyp.6851

Chow VT (1964) Handbook of applied hydrology: a compendium of water-resources technology. McGraw-Hill, Inc, 1468 pages. ISBN-13: 978–0070107748

Deutsch CV (1996) Correcting for negative weights in ordinary kriging. Comput Geosci 22(7):765–773. doi:10.1016/0098-3004(96)00005-2

Eagleson PS (1967) Optimum density of rainfall networks. Water Resour Res 3(4):1021–1033. doi:10.1029/WR003i004p01021

Goovaerts P (2000) Geostatistical approaches for incorporating elevation into the spatial interpolation of rainfall. J Hydrol 228(1–2):113–129. doi:10.1016/S0022-1694(00)00144-X

Haberlandt U (2007) Geostatistical interpolation of hourly precipitation from rain gauges and radar for a large-scale extreme rainfall event. J Hydrol 332(1–2):144–157. doi:10.1016/j.jhydrol.2006.06.028

Hongliang X, Chong-YX NRS, Youpeng X, Bin Z, Hua C (2015) Entropy theory based multi-criteria resampling of rain gauge networks for hydrological modelling—a case study of humid area in southern China. J Hydrol 525:138–151. doi:10.1016/j.jhydrol.2015.03.034

Hui-Chung Y, Chen YC, Wei C, Chen RH (2011) Entropy and kriging approach to rainfall network design. Paddy Water Environ 9(3):343–355. doi:10.1007/s10333-010-0247-x

Isaaks EH, Srivastava RM (1989) An introduction to applied geostatistics. Oxford University Press, New York 561 pp. ISBN-13: 978-0195050134

Johnston K, VerHoef JM, Krivoruchko K, Lucas N (2001) Using ArcGIS geostatistical analyst. ArcGIS Manual by ESRI, Redlands

Kar AK, Lohani AK, Goel NK, Roy GP (2015) Rain gauge network design for flood forecasting using multi-criteria decision analysis and clustering techniques in lower Mahanadi River basin, India. J Hydrol Reg Stud 4(part B):313–332. doi:10.1016/j.ejrh.2015.07.003

Kassim AHM, Kottegoda NT (1991) Rainfall network design through comparative kriging methods. Hydrol Sci J 36(3):223–240. doi:10.1080/02626669109492505

Krajewski WF (1987) CoKriging radar-rainfall and rain gage data. J Geophys Res 92(D8):9571–9580. doi:10.1029/JD092iD08p09571

Langbein WB (1960) Hydrologic data networks and methods of extrapolating or extending available hydrologic data, in Hydrologic Networks and Methods. United Nation, ECAFF/WMO Flood Control Series No 15, 15:12–41

Lloyd CD (2005) Assessing the effect of integrating elevation data into the estimation of monthly precipitation in Great Britain. J Hydrol 308(1–4):128–150. doi:10.1016/j.jhydrol.2004.10.026

Ly S, Charles C, Degre A (2011) Geostatistical interpolation of daily rainfall at catchment scale: the use of several variogram models in the Ourthe and Ambleve, catchments, Belgium. Hydrol Earth Syst Sci 15:2259–2274. doi:10.5194/hess-15-2259-2011

Mahmoudi-Meimand H, Nazif S, Abbaspour RA, Sabokbar HF (2015) An algorithm for optimisation of a rain gauge network based on geostatistics and entropy concepts using GIS. J Spat Sci 61(1):233–252. doi:10.1080/14498596.2015.1030789

Pardo-Igúzquiza E (1998) Optimal selection of number and location of rainfall gauges for areal rainfall estimation using geostatistics and simulated annealing. J Hydrol 210(1–4):206–220. doi:10.1016/S0022-1694(98)00188-7

Patra KC (2001) Hydrology and water resources engineering. Alpha Science: Pangbourne ISBN-13: 978–1842654217

Seo DJ, Ridwan S, Peter A (2015) Objective reduction of rain gauge network via geostatistical analysis of uncertainty in radar-gauge precipitation estimation. J Hydrol Eng 20(4). doi:10.1061/(ASCE)HE.1943–5584.0000969, 04014050 04014050

St-Hilaire A, Ouarda TBMJ, Lachance M, Bob'ee B, Gaudet J, Gignac C (2003) Assessment of the impact of meteorological network density on the estimation of basin precipitation and runoff: a case study. Hydrol Process 17(18):3561–3580. doi:10.1002/hyp.1350

Teegavarapu R, Chandramouli V (2005) Improved weighting methods, deterministic and stochastic data-driven models for estimation of missing precipitation records. J Hydrol 312(1–4):191–206. doi:10.1016/j.jhydrol.2005.02.015

Tsintikidis D, Georgakakos KP, Sperfslage JA, Smith DE, Carpenter TM (2002) Precipitation uncertainty and rain gauge network design within Folsom Lake watershed. J Hydrol Eng 7(2):175–184. doi:10.1061/(ASCE)1084-0699(2002)7:2(175)

Vicent-Serrano SM, Saz-Sanchez MA, Cuadrat JM (2003) Comparative analysis of interpolation methods in the middle Ebro Valley (Spain): application to annual precipitation and temperature. Clim Res 24(2):161–180. doi:10.3354/cr024161

Webster R, Oliver MA (2007) Geostatistics for environmental scientists, statistics in practice series, 2nd ed. John Wiley & Son Ltd. p 315–330. ISBN: 978–0–470-02858-2

WMO (2008) World Meteorological Organization guide to hydrological practices, sixth edn. WMO-168 WMO, Geneva